Traveling pulses in anisotropic oscillatory media with global coupling

M. Falcke and H. Engel
Institut für Theoretische Physik, Technische Universität Berlin, Hardenbergstrasse 36, 10623 Berlin, Germany
(Received 7 May 1996)

The CO oxidation on the (110) surface of a platinum single crystal has a strongly state dependent diffusion anisotropy. The surface is coupled globally through the gas phase. We consider the oscillatory regime. The dependence of the anisotropy on the surface structure is modeled by a cubic equation. We have found, that diffusion driven traveling pulses in the oscillatory regime—so-called phase flips—can arise from a small phase gradient under global coupling. Anisotropy causes five different regimes of the expansion of phase flips and spiral formation. The spiral formation additionally depends on the direction of the rotation of the spiral. [S1063-651X(97)14006-5]

PACS number(s): 82.20.Wt, 82.20.Mj, 82.65.Jv

I. INTRODUCTION

Dynamical systems obeying nonlinear ordinary differential equations can show different regimes of dynamical behavior in dependence on their parameters. Those regimes are, for instance, bistability, excitability, and the oscillatory regime. In the last one the physical variables steadily oscillate. In the bistable regime the system stays in one stable stationary state until a supercritical perturbation causes a transition to the other stable stationary state. In the excitable regime the unperturbed system stays in the stable stationary state, until a supercritical perturbation leads first to a strong amplification of the perturbation and finally to a relaxation to the stable state.

In spatially extended chemical systems, described by nonlinear partial differential equations, certain wave phenomena belong to these regimes. Fronts of transition from one stable state to the other are typical for the bistable regime [1]. In the excitable regime pulses occur. They appear as straight pulses, as target patterns generated by a pacemaker in their center, or as spiral waves [2–4]. Target pattern and spirals exist also in oscillatory media. For these spatial patterns again different regimes occur depending on the values of the parameters specifying the local dynamical regime [2,3,5,6]. For instance, in the excitable regime spiral waves exist only above certain critical values for diffusion or excitability. At parameters below these critical values every pulse with an open end would shrink and finally vanish or pulses would not occur at all. These regimes of wave propagation have been widely investigated for isotropic conditions. Recently, some investigations have been done for anisotropic excitable chemical media [7–9]. The crucial property of the investigated anisotropy is, that it is dependent on one dynamic variable and therefore cannot be eliminated from the equations by a simple rescaling of the space coordinates. We are interested here in different regimes for the expansion of pulses in a two-dimensional anisotropic medium in the oscillatory regime. These conditions apply to CO oxidation on Pt(110) single crystal surfaces. In this system the anisotropy depends on the inhibitor variable.

Besides local spatial coupling by surface diffusion of adsorbed species, the CO oxidation on Pt(110) surfaces is globally coupled. The partial pressure of carbon monoxide provides the global coupling through the gas phase. Changes of partial pressure influence the local dynamics, which forms the spatial pattern. Conversely the spatial pattern governs the average adsorption and desorption of carbon monoxide on which the strength of the global coupling depends. In this way the spatial pattern of adsorbates on the Pt surface and the global coupling interact. We will consider this interaction in this paper as well.

II. THE MODEL

The model starts from a kinetic scheme that has been proposed by Krischer, Eiswirth, and Ertl [10]

$$\frac{\partial C}{\partial t}=D_1\frac{\partial^2 C}{\partial r_1^2}+\frac{\partial}{\partial r_2}\left(D_2(W)\frac{\partial C}{\partial r_2}\right)+k_1 p_{\mathrm{CO}} s_c\left[1-\left(\frac{C}{c_s}\right)^3\right]-k_2 C-k_3\mathrm{CO}, \tag{1}$$

$$\frac{\partial O}{\partial t}=k_4 p_{02}[(s_{01}-s_{02})W+s_{02}]\left(1-\frac{C}{c_s}-\frac{O}{o_s}\right)^2-k_3\mathrm{CO} \tag{2}$$

$$\frac{\partial W}{\partial t}=k_5\begin{cases}-W, & 0\leqslant\dfrac{C}{c_s}<0.2\\[2ex] -W-\dfrac{\left(\dfrac{C}{c_s}\right)^3-1.05\left(\dfrac{C}{c_s}\right)^2+0.3\dfrac{C}{c_s}-0.026}{0.0135}, & 0.2\leqslant\dfrac{C}{c_s}\leqslant 0.5\\[2ex] -W+1, & 0.5<\dfrac{C}{c_s}\leqslant 1.0\end{cases}$$
$$=k_5\left[g\left(\frac{C}{c_s}\right)-W\right]. \tag{3}$$

Table I lists the variables and parameters of the equations. Equation (1) for the coverage of carbon monoxide C describes adsorption and desorption of CO and also the formation of CO_2 according to the Langmuir-Hinshelwood mechanism [10]. The balance of oxygen coverage O—Eq. (2)—includes the adsorption and reaction terms. We may ignore contributions due to desorption and to diffusion in the parameter range considered. The kinetic scheme involves an adsorbate-driven phase transition of the Pt(110) surface between a 1×2 structure of the clean surface and a 1×1

TABLE I. Parameters and variables.

		Variables	
	C	CO coverage	
	O	O coverage	
	W	fraction of the surface in the 1×1 structure	
	p_{CO}	partial pressure of CO	
		Parameters	
CO	k_1	adsorption rate	4.18×10^5 ML s^{-1} $Torr^{-1}$
	s_c	sticking coefficient	1
	c_s	saturation coverage	1 ML
O_2	k_4	adsorption rate	7.81×10^5 ML s^{-1} $Torr^{-1}$
	s_{01}	sticking coefficient on 1×1	0.6
	s_{02}	sticking coefficient on 1×2	0.4
	o_s	saturation coverage	0.8 ML
		Rates with $k_i=A_i\exp(-E_i/RT)$	
k_3	reaction	$A_3=3\times10^6$ (ML s)$^{-1}$, $E_3=10$ kcal/mol	
k_2	CO desorption	$A_2=2\times10^{16}$ s^{-1}, $E_2=38$ kcal/mol	
k_5	phase transition	$A_5=200$ s^{-1}, $E_5=7$ kcal/mol	
		Diffusion (local coupling)	
D_1	diffusion coefficient in the (110) direction: 10 $\mu m^2/s$		
$D_2(W)$	diffusion coefficient in the (001) direction: depends on W		
		Gas phase coupling (global coupling)	
V	reactor volume: 55 l		
J_{i0}	volume current into the reactor: 360 l s^{-1}		
A	crystal surface		
V_{ML}	volume of one monolayer adsorbed CO: 0.3–0.81 ML^{-1}		
p_{COE}	partial pressure of CO in the gas inlet: 4×10^{-5} Torr		
		Control parameters	
T	temperature: 545 K		
p_{02}	partial pressure of oxygen		

structure of the CO covered surface. Equation (3) describes this process. W is the fraction of the surface in the 1×1 structure.

The transition of the surface structure leads to a dependence of the diffusion coefficient on W in the (001) crystallographic direction D_2

$$D_2(W)=D_2\left[1+\left(\frac{D_1}{D_2}-1\right)W^3\right]=D_2\rho(\zeta,W),\quad \zeta=\frac{D_1}{D_2}. \tag{4}$$

Equation (4) is an ansatz for the dependence of D_2 on W. Let us assume $D_2 \ll D_1-D_2$. Then the ratio of the maximum of the diffusion coefficient to its minimum $D_{2,\max}/D_{2,\min}$ depends on $(W_{\max}/W_{\min})^3$. Because $(W_{\max}/W_{\min})$ is about 2, the exponent 3 provides $D_{2,\max}/D_{2,\min}\approx 8$. This is in the range of the experimental observations [11]. The crucial zone of a pulse for the diffusion processes is the pulse front. It is a very thin layer, because the system (1)–(3) oscillates with relaxation oscillations. W changes only a little in the front because its typical time scale is much larger than that of C. To get an impact of the change of W on the diffusion inside the front, the dependence of D_2 on W has to be sensitive enough. The cubic dependence supplies this sensitivity.

Adsorption and desorption of CO produce local differences of the partial pressure of carbon monoxide p_{CO}. Differences balance immediately (within 10^{-3} s) compared to the time scale of the oscillations (~ 5 s). In this way a global coupling arises. The balance equation for the partial pressure of carbon monoxide is

$$\frac{dp_{\mathrm{CO}}}{dt}=\frac{J_{io}}{V}\left[p_{\mathrm{CO}E}-p_{\mathrm{CO}}\left(1+\frac{V_{\mathrm{ML}}}{J_{io}}\int_A\frac{dr^2}{A}\left\{k_1 p_{\mathrm{CO}}\left[1-\left(\frac{C}{c_s}\right)^3\right]-k_2\left(\frac{C}{c_s}\right)\right\}\right)\right]. \tag{5}$$

Equation (5) allows for the gas supply, exhaust, and the adsorption and desorption. $p_{\mathrm{CO}E}$ is the partial pressure of carbon monoxide in the gas inlet, for the other parameters see Table I. The value of the amplitude of the p_{CO} oscillations is the strength of the global coupling, because the larger the oscillations of the global variable p_{CO} the larger their influence is on the local dynamics. The p_{CO} oscillation amplitude is proportional to V_{ML} for small V_{ML}—especially for the whole existence range of phase flips discussed below. Therefore we can consider V_{ML} as a measure for the strength of global coupling and use it as a bifurcation parameter. We expect similar results when experimentally adjustable parameters as the partial pressure of oxygen p_{O2}, for example, are chosen appropriately.

The strength of the global coupling depends on the spatial pattern on the crystal surface, too. For instance, the one-dimensional pattern $C=C_0(t)\cos(2\pi r/S)$ would lead to a constant value of the integral in Eq. (5) and there would be no p_{CO} oscillations. The homogeneous oscillating state is the pattern with the largest amplitudes of the p_{CO} oscillations and, therefore, with the strongest global coupling.

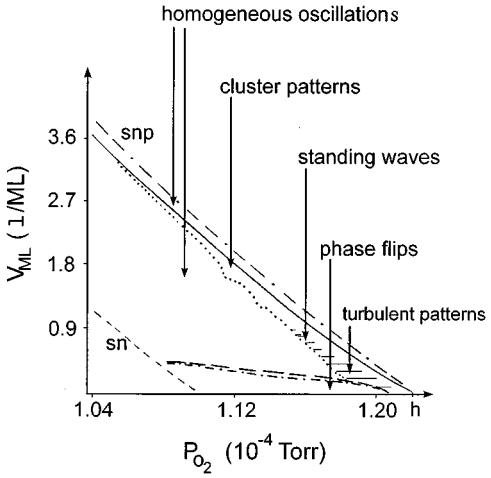

FIG. 1. Bifurcation scheme of the spatiotemporal structures of the globally coupled reconstruction model in the $p_{02}-V_{\mathrm{ML}}$-parameter plane. h: supercritical Hopf bifurcation, sn$p$: saddle-node bifurcation of limit cycles, sn: saddle-node bifurcation. Full line: upper boundary of the region with cluster patterns; hatched area: irregular patterns; dotted line: lower boundary of the range with irregular resp. cluster patterns; long-dashed line: upper boundary for the existence of phase flips traveling in (001) direction; dashed-dotted line: upper boundary for the existence of phase flips traveling in $(1\,\overline{1}\,0)$ direction. Standing waves exist in the transition range between turbulent patterns and cluster patterns. The procedure used for the determination of the lines is explained in [5].

We keep the following parameters constant through all calculations in this paper: $T=545$ K, $p_{\mathrm{CO}E}=4\times10^{-5}$ Torr, $J_{io}=360$ ls^{-1}, $V=55$ l, and $D_1/D_2=8$.

III. NUMERICAL METHODS

The partial differential equations have been integrated semi-implicitly, by which we mean that the reaction part was treated implicitly and the diffusion part explicitly. The diffusion term was calculated using the formulas given in [12] forming the spatial derivative of the diffusion coefficient numerically. We integrated Eq. (5) explicitly. The spatial integration has been performed with a procedure of order $\mathrm{O}(1/N^4)$ (where N is the number of grid points in one dimension).

IV. RESULTS

We have investigated the pattern formation in the $p_{02}-V_{\mathrm{ML}}$-parameter plane. Five different patterns have been found: the homogeneous oscillating state, turbulent patterns, cluster patterns, standing waves, and phase flips (see Fig. 1). References [5,13–15] describe the first four. We focus on the phase flips here.

Phase flips are diffusion driven waves in oscillatory media. We want to use the phase picture of oscillatory systems to characterize the phase flips. The state of an oscillatory system moving on a limit cycle can be completely described by a phase variable ϕ [16]. ϕ is the position on the limit cycle and $\phi=2\pi$ corresponds to one whole rotation. In spatially extended systems ϕ depends on the space coordinate r: $\phi=\phi(r,t)$. Phase flips are phase fronts with a height of

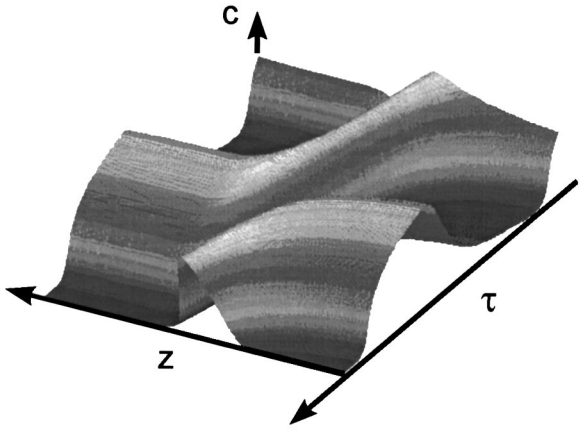

FIG. 2. One-dimensional phase flip in dependence on dimensionless space coordinate z and dimensionless time τ. The symmetry in space and time dependence is obvious.

2π and a space-time dependence of the form: $\phi(r,t)=\phi(r-st)$ (see Fig. 2 also). Here s denotes the velocity of the front.

Phase flips can arise from a phase wave. Initially the phase gradient $\Delta\phi$ producing the phase wave can be quite flat. The gradient becomes amplified and more localized by the global coupling. During this process the velocity of the phase wave decreases because it is proportional to $(\Delta\phi)^{-1}$. At a certain value of $\Delta\phi$ the phase wave turns into a diffusion driven wave—the phase flip—with a constant velocity and a constant value of $\Delta\phi$ (see [17] and Fig. 3). The amplification occurs if in the absence of local coupling $(D_1=D_2=0)$ only the homogeneous oscillating state is stable.

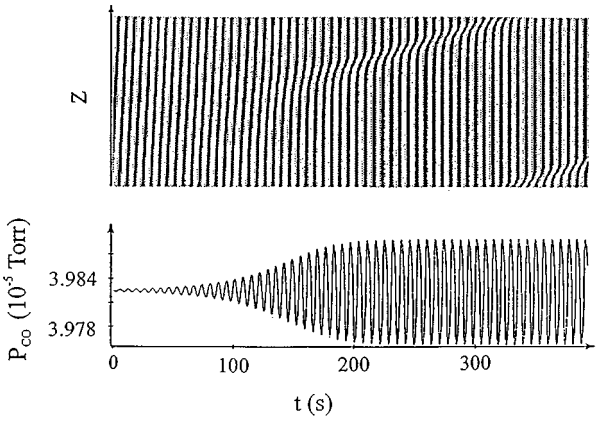

FIG. 3. Formation of a one-dimensional phase flip in space (length of the z area about 600 μm) and time t. Below the partial pressure of CO is shown as a function of time at $p_{02}=1.16\times10^{-4}$ Torr, $V_{ML}=0.17$ 1/ML. The initial condition is a phase gradient $\Delta\phi=2\pi/L$ (L—system length). The velocity of this initial phase wave is L/T_0 (T_0—period of oscillations). The phase gradient becomes steeper and more localized by the global coupling and its velocity decreases down to $L/(67T_0)$. During this process the global coupling becomes stronger (p_{CO}—amplitudes increase), because the initial condition has almost no homogeneous Fourier components and the stationary state has a homogeneous component with large amplitude.

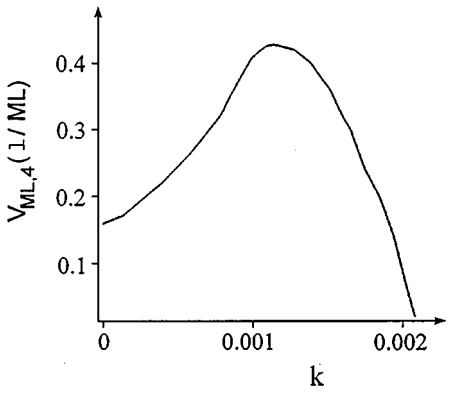

FIG. 4. Upper boundary for the existence of phase flips traveling in $(1\,\bar{1}\,0)$ direction in dependence on the wave vector k at $p_{02}=1.17\times10^{-4}$ Torr. The maximum wave vector is about 0.0012 in dimensionless units; this corresponds to a wave length of about 90 μm.

Not only can the global coupling create the phase flips, but also the phase flips can influence the global coupling. Periodic trains of phase flips weaken the global coupling. The reason is the decreasing amplitude of the oscillations of the spatial average of adsorption and desorption in Eq. (5). That is why the upper existence boundary of the phase flips on the V_{ML} axis—$V_{ML,4}$—increases, if the wave vector k of the trains of phase flips increases (see Fig. 4). $V_{ML,4}$ drops at large k, because the minimal wave length at which phase flips can exist is reached. Therefore the local coupling by diffusion causes that drop.

The most obvious consequence of the anisotropy on the Pt(110) surface is a dependence of the pulse velocity on the direction. The ratio between the velocity in the $(1\,\bar{1}\,0)$ direction and (001) direction is equal to $(D_1/D_2)^{1/2}$ with constant anisotropy. In our case it is a little less, because the diffusion in (001) direction is almost always larger than D_2.

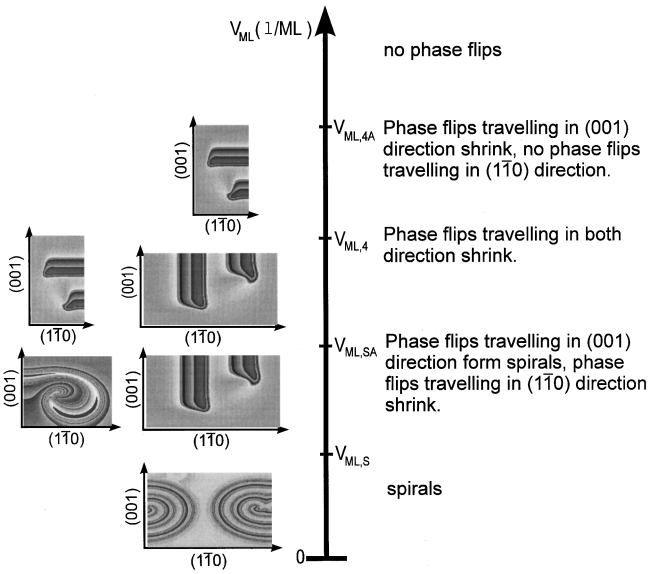

FIG. 5. Regimes of expansion of phase flips in dependence on V_{ML} at $p_{02}=1.16\times10^{-4}$ Torr: $V_{ML,S}=0.132$ 1/ML, $V_{ML,SA}=0.157$ 1/ML, $V_{ML,4}=0.176$ 1/ML, and $V_{ML,4A}=0.215$ 1/ML.

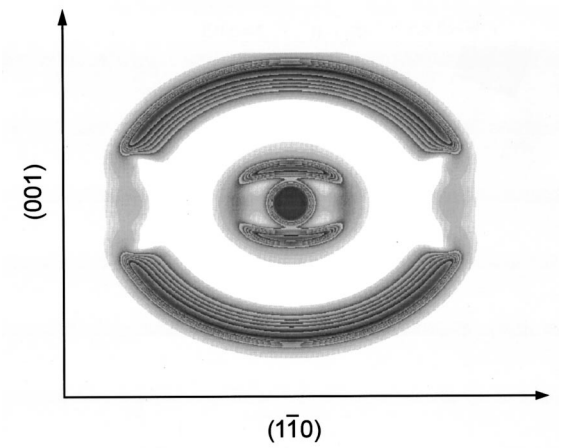

FIG. 6. Broken target pattern at $V_{ML,4}<V_{ML}<V_{ML,4A}$. The carbon monoxide concentration is shown. The brighter the gray level is, the higher is the concentration value. The parameters are $V_{ML}=0.18$ 1/ML and $p_{02}=1.16\times10^{-4}$ Torr. Size of the imaged area: 610 μm $\times$520 μm.

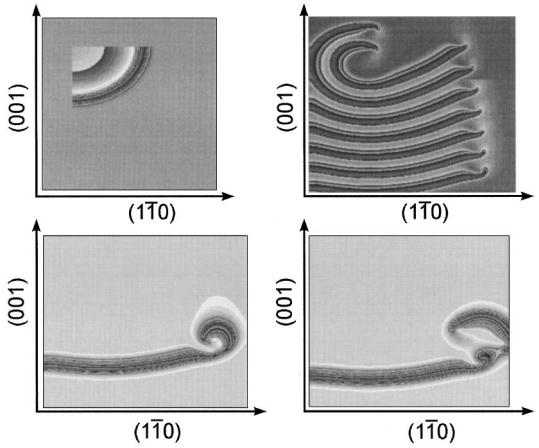

FIG. 7. Alignment of a phase flip in the regime $V_{ML,S}<V_{ML}<V_{ML,SA}$. The carbon monoxide concentration is shown. The brighter the gray level is, the higher is the concentration value. The upper left picture shows the initial condition. The upper right picture shows the phase flip after 19, 25, 31, 37, 43, 49, and 55 periods of the oscillation. The lower left picture shows the beginning of a spiral after 64 periods. The lower right picture shows, how a part of the spiral splits off and the phase flip forms a new spiral, which will be stable. The parameters are $V_{ML}=0.14$ 1/ML and $p_{02}=1.16\times10^{-4}$ Torr. Size of the imaged area: 870 μm $\times$740 μm, upper left: 740 μm $\times$740 μm.

For the following discussion we define the term ''direction of an open end.'' The direction of an open end is the direction perpendicular to the pulse front at the open end. For instance, the open end on the left-hand side of the initial condition in the upper left picture of Fig. 7 is directed in the (001) direction.

There are five different regimes for the evolution of phase flips in dependence on V_{ML} (compare Fig. 5). Above $V_{ML,4A}$ no pulses can exist and the homogeneous oscillating state is the only stable regime.

The anisotropy causes the other four regimes. For $V_{ML,4}<V_{ML}<V_{ML,4A}$, pulses can travel only in the (001) direction, and if they have an open end, they shrink. A two-dimensional pattern that can occur in this regime is shown in Fig. 6. A pacemaker creates a ring of a target pattern. The ring breaks where its front is perpendicular to the $(1\,\bar{1}\,0)$ direction. Both remaining parts of the ring travel in the (001) direction until their length shrinks to zero.

For V_{ML} between $V_{ML,S}$ and $V_{ML,SA}$ phase flips can travel in both directions, but only phase flips traveling in the (001) direction can form spirals. The two dimensional structures occurring in this regime are target pattern and spirals. Before a pulse with an open end forms a spiral, it aligns in the $(1\,\bar{1}\,0)$ direction. That is why the connecting line of the core centers of a double spiral is always directed approximately in the $(1\,\bar{1}\,0)$ direction in this regime. Figure 7 shows the alignment process. Starting from a bended pulse cut out of a target pattern, it takes more than 64 oscillation periods until a spiral develops. The alignment is caused by the dependence of the velocity on the direction. The pulse aligns vertical to the direction with the smallest velocity—the (001) direction. Another condition for the alignment is, that the open end initially directed into the $(1\,\bar{1}\,0)$ direction cannot grow into the (001) direction, respectively, form a spiral.

Figure 8 shows the results of a simulation with an open end directed in a direction with an angle between 0 and 90 degrees to the $(1\,\bar{1}\,0)$ direction. The crucial difference to the simulation in Fig. 7 is, that the initial rotation of the spiral turns the open end into the (001) direction, whereas the spiral in Fig. 8 turns the open end initially in the $(1\,\bar{1}\,0)$ direction. The open end of the pulse in Fig. 7 pointed during the process of alignment at a certain time in the same direction as the open end of the initial condition in Fig. 8, but did not start to form a spiral. That shows, that the development of a spiral not only depends on the direction of the open end but also on the direction in which the open end had to turn to form a spiral.

For the spiral formation with an initial turn into the (001) direction we have found a critical angle θ_{cr}. If the open end is initially directed with an angle smaller than θ_{cr}, it shrinks. Otherwise, it forms a spiral. At our standard parameters, $p_{02}=1.16\times10^{-4}$ Torr and $V_{ML}=0.14$ 1/ML we find

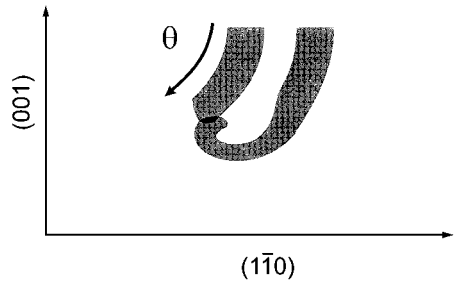

FIG. 8. Spiral formation with a phase flip turning the open end initially into the (001) direction at $V_{ML,S}<V_{ML}<V_{ML,SA}$. The parameters are $V_{ML}=0.14$ 1/ML and $p_{02}=1.16\times10^{-4}$ Torr. The phase flip on the left-hand side is the initial condition, this one on the right-hand side is the state after seven oscillation periods. The initial condition has been cut out of an elliptical target pattern. At the upper end the normal of the initial condition points into the $(1\,\bar{1}\,0)$ direction. The normal of the other end has an angle θ with this direction.

$\theta_{cr}=0.122\pi$. We did not determine more values of θ_{cr}, because of the large amount of two-dimensional integrations required, but it seems plausible, that θ_{cr} increases from 0 to $\pi/2$ as V_{ML} increases from $V_{ML,S}$ to $V_{ML,SA}$, because at $V_{ML,S}$ all pulses form a spiral and at $V_{ML,SA}$ no pulse can form a spiral.

Finally there is the regime at $V_{ML}<V_{ML,S}$, in which phase flips can travel in both directions and can form spirals without any restriction. Spirals and target patterns are the two-dimensional structures occurring in this parameter range.

V. DISCUSSION

Phase flips in oscillatory active media subjected to external periodic forcing have first been considered by Coullet and Emilsson, who noted their similarity to traveling pulses in excitable media [18,19].

We have investigated phase flips in a system with state dependent anisotropy and global coupling modeling the CO oxidation on Pt(110) surfaces. The global coupling is able to create phase flips out of a weak phase gradient. This is possible because those phase gradients generate spatial concentration profiles with small wave vectors, which do not destroy the global coupling.

Our aim was to investigate pattern formation under global coupling in continuation of the work presented in Refs. [6,13,14]. We have found five different regimes for the propagation of phase flips. They are with decreasing V_{ML}: no phase flips, shrinking phase flips in the (001) direction, shrinking phase flips in both directions, spiral forming phase flips in the (001) direction, shrinking phase flips in the $(1\bar{1}0)$ direction, and, finally, spiral forming phase flips in both directions. The results show which different regimes of pulse propagation may occur in oscillatory media. Mertens *et al.* provide analogous results for traveling wave fragments in excitable media with complex anisotropy [9].

We used V_{ML} as the bifurcation parameter considering this parameter as a measure of the strength of global coupling, because it is proportional to the amplitude of oscillations of the partial pressure of CO in the gas phase. We expect similar results when the partial pressure of oxygen or another experimentally adjustable parameter is chosen appropriately. Anyway, the parameter window of the observed behavior is small.

A systematic experimental investigation of the influence of state-dependent anisotropy was done only for the reduction of NO with H_2 on Rh(110) surfaces. The phenomena found there agree with our results only with respect to the existence of a preferred direction of the pulse velocity [8,9]. The Pt(110) surface shows this preferred direction as well in a certain regime of parameters [20]. The major difference to our results is, that the experimentally observed pulses show a constant length, whereas our model predicts only shrinking pulses. In the regime between $V_{ML,S}$ and $V_{ML,SA}$ the axis connecting the cores of a double spiral emerged from both ends of the same pulse should be directed in the direction of constant diffusion. Further consequences of the anisotropy are the elliptical shape of spirals and target patterns and a certain orientation of standing waves in the oscillatory regime. The latter is discussed in [5].

Phase flips in the (001) direction with diffusion depending on the surface structure turn out to be more stable than phase flips in the $(1\bar{1}0)$ direction with constant stronger diffusion. We suppose, that this can be explained by similar phenomena in excitable media. Gottschalk reports in [21] a decrease of the stability of pulses in the excitable regime, if the diffusion increases inside the excited part of the pulse. He explains, that with increasing diffusion the back front of the pulse catches up to the front and the pulse becomes shorter or collapses.

According to Mertens, Imbihl, and Mikhailov [22] trains of phase flips can lead to a breakdown of global coupling. In this situation periodic traveling phase flips represent only transient states of the system. In [22] this was described in the framework of the globally coupled complex Ginzburg-Landau equation. As mentioned above, the reason for this behavior is the spatially averaging character of the oscillations of the global variable. If the spatial profile of the phase flip has no spatially homogeneous Fourier component and the coupling term is linear, like in the globally coupled complex Ginzburg-Landau equation, any phase flip will destroy the global coupling. On the contrary, in the case discussed here there is a homogeneous Fourier component in the spatial profile of a phase flip, and the coupling term is an integral over a nonlinear function of the concentration [compare Eq. (5)]. We have finite oscillations of the global variable at small wave vectors. From our calculation it follows that then periodic trains of phase flips weaken the global coupling but do not trigger its complete breakdown.

In the considered parameter range the strength of the global coupling is proportional to V_{ML} and the global coupling acts as a homogenizing force. That leads to the creation of phase flips on the one hand and to the breakdown of the phase flips at high V_{ML} on the other hand.

ACKNOWLEDGMENTS

This work was partially supported by a grant from the Deutsche Forschungsgemeinschaft and the Fonds der Chemischen Industrie.

[1] R. J. Field and M. Burger, *Oscillations and Traveling Waves in Chemical Systems* (Wiley, New York, 1985).
[2] A. Winfree, CHAOS **1**, 303 (1991).
[3] M. Bär and M. Eiswirth, Phys. Rev. E **48**, R1635 (1993).
[4] H. H. Rotermund, S. Jakubith, A. v. Oertzen, and G. Ertl, Phys. Rev. Lett. **66**, 3083 (1991).
[5] M. Falcke, H. Engel, and M. Neufeld, Phys. Rev. E **52**, 763 (1995).
[6] M. Falcke, M. Bär, H. Engel, and M. Eiswirth, J. Chem. Phys. **97**, 4555 (1992).
[7] A. Mikhailov, Phys. Rev. E **49**, 5875 (1994).
[8] N. Gottschalk, F. Mertens, M. Bär, M. Eiswirth, and R. Imbihl,

Phys. Rev. Lett. **73**, 3483 (1994).
[9] F. Mertens, N. Gottschalk, M. Bär, M. Eiswirth, and A. Mikhailov, Phys. Rev. E **51**, R5193 (1995).
[10] K. Krischer, M. Eiswirth, and G. Ertl, Surf. Sci. **900**, 251 (1991).
[11] S. Jakubith, H. H. Rotermund, W. Engel, A. von Oertzen, and G. Ertl, Phys. Rev. Lett. **65**, 3013 (1990).
[12] W. H. Press, B. P. Flannery, S. A. Teukolsky, and W. T. Vetterling, *Numerical Recipes in C* (Cambridge University Press, Cambridge, England, 1988), pp. 600 and 661.
[13] M. Falcke and H. Engel, J. Chem. Phys. **101**, 6255 (1994).
[14] M. Falcke and H. Engel, Phys. Rev. E **50**, 1353 (1994).
[15] M. Bär, M. Eiswirth, H. Engel, M. Falcke, M. Hilderbrand, and M. Neufeld, CHAOS **4**, 499 (1994).
[16] Y. Kuramoto, *Chemical Oscillations, Waves and Turbulence* (Springer, Berlin, 1984).
[17] E. J. Reusser and R. J. Field, J. Am. Chem. Soc. **101**, 1063 (1979).
[18] P. Coullet and K. Emilsson, Physics A **188**, 190 (1992).
[19] P. Coullet and K. Emilsson, Physica D **61**, 119 (1992).
[20] M. Bär, M. Eiswirth, H.-H. Rotermund, and G. Ertl, Phys. Rev. Lett. **69**, 945 (1992).
[21] N. Gottschalk, Ph.D. thesis, Technische Universität Berlin, 1994 (unpublished).
[22] F. Mertens, R. Imbihl, and A. Mikhailov, J. Chem. Phys. **99**, 8668 (1993).